Indian Journal of Biochemistry & Biophysics
Vol. 62, January 2025, pp. 17-24
DOI: 10.56042/ijbb.v62i1.13885

The HMG-CoA reductase inhibitory potential of fatty acid amides

Meran Keshawa Ediriweera[1]*, Joshua Miguel Anandappa[2] & Baohua Zhang[3]*

[1]Department of Biochemistry and Molecular Biology, Faculty of Medicine, University of Colombo, Colombo-08, Sri Lanka

[2]Department of Biomedical Science, BMS School of Science, Colombo-06, Sri Lanka

[3]Computer Network Information Center, Chinese Academy of Sciences, Beijing, China

Received 21 September 2024; *revised 08 October 2024*

HMG-CoA reductase (HMGCR) plays a key role as the rate-limiting enzyme in cholesterol biosynthesis. Fatty acid amides possess a range of biochemical and physiological functions. In an attempt to identify potential inhibitors of HMGCR, three fatty acid amides - namely stearamide, oleamide, and butyramide were investigated. Results demonstrated that these amides inhibited the activity of HMGCR, with stearamide being the most potent, followed by oleamide and butyramide. Stearamide appears to demonstrate a competitive mode of inhibition for HMGCR. Notably, these fatty acid amides interacted with key amino acid residues in the catalytic region of HMGCR through hydrogen bonding and hydrophobic interactions. These findings highlight the necessity for further research to delve into the effects of fatty acid amides on HMGCR inhibition in both *in vitro* and *in vivo*.

Keywords: Butyramide, Cholesterol biosynthesis inhibition, Enzyme assays, Oleamide, Stearamide

3-hydroxy-3-methylglutaryl-coenzyme A reductase (HMGCR) is an enzyme that plays a key role in the cholesterol biosynthesis pathway. As the rate-limiting enzyme in this pathway, it is essential for maintaining cholesterol homeostasis[1]. The primary fatty acid amides derived from oleic, palmitic, palmitoleic, elaidic and linoleic fatty acids exhibit a wide range of physiological roles[2]. Oleamide is a fatty acid amide derived from oleic acid. It is found in human serum[3,4] and in human cancer cells[5]. The occurrence of oleamide has also been reported in human meibomian glandsecretions[6]and in plants[7]. One of its prominent roles is its influence on sleep regulation, as it has been shown to induce sleep[8]. Oleamide inhibits gap junction communication[9] and triggers the biological effects of $GABA_A$ receptor and several subtypes of serotonin receptor, including 5-HT1A, 5-HT2A, and 5-HT2C[10]. Additionally, antioxidant properties[11], which contribute to its potential therapeutic applications. Recently, oleamide has been identified as a as potential circulating biomarkers for sarcopenia[12].

Stearamide is a fatty acid amide of steric acid. Like oleamide, stearamide is also present in human[4,6] and plants[13]. In addition, the fatty acid amides oleamide and stearamide have been identified as potential biomarkers for neurodegenerative and liver diseases[4,14]. Butyramide is derived from butyric acid. The epigenetics effects of butyric acid and some butyramide derivatives have been well established[15]. Investigations reported in the early nineties demonstrated that, phenyl butyramide, a butyric acid derivative, can reduce cholesterol levels or biosynthesis[16]. In light of the limited studies exploring the direct biological impact of fatty acid amides on HMGCR activity, we undertook this study to examine the effects of three selected fatty acid amides, oleamide, stearamide, and butyramide, on this rate-limiting enzyme of cholesterol biosynthesis.

Materials and Methods

Chemicals and kits

The fatty acid amides oleamide (Cat. No. O2136), stearamide (Cat. No. 89884) and butyramide (Cat. No. 19240) and the HMGCR assay kit (CS1090) and HMG-CoA (H6132) were purchased from Sigma-Aldrich, USA. Stock solutions of fatty acid amides were prepared in ethanol.

HMG-COA reductase (HMGCR) assay

The HMGCR assay kit measures the activity of HMGCR, an important enzyme involved in cholesterol biosynthesis. This kit utilizes a

*Correspondence:
Phone: +94779960397 (Mob)
E-mail: meran@bmb.cmb.ac.lk; mk.ediriweera@gmail.com (MKE); zhangbh@sccas.cn (BZ)

colorimetric assay principle, utilizing the conversion of HMG-CoA to mevalonate by HMGCR. The change in absorbance is indicative of the oxidation of NADPH by the catalytic subunit HMGCR when the substrate HMG-CoA is present. In the assay, fatty acid amides were tested at two concentrations: 25 and 50 µM. For inhibition assays, the reactions were prepared by mixing 2 µL of HMGCR, 12 µL HMG-CoA, 181 µL of 1X assay buffer, 4 µL of NADPH and 1 µL of fatty acid amides from stock solutions in 96-well plates. Reaction controls received no fatty acid amides. The effects of fatty acid amides on the activity of HMGCR was determined by measuring the colour produced by the reaction in a microplate reader using a kinetics program at 340 nm. The readings were taken for 15 min at 30 sec time intervals with vigorous shaking. The percentage enzyme inhibition was calculated using the following equation (between 540-900 sec in spectrophotometric time scans):

Percentage enzyme inhibition = (ΔAbs/ΔT (enzyme control)- ΔAbs/ΔT (enzyme + fatty acid amide)/ ΔAbs/ΔT (enzyme control) x 100[17,18]

Kinetic study

To determine the kinetic properties of HMGCR, three concentrations of HMG-CoA (0.3, 0.6, and 0.9 mM), the substrate of HMGCR, were used in the absence and presence of a single concentration of 25 µM of stearamide, the amide that showed the greatest inhibitory potential. The inhibition mode was determined by double-reciprocal Lineweaver-Burk plot analysis according to Michaelis-Menten kinetics and K_m and V_{max} values were determined.

Receptor and ligand preparations and molecular docking

Receptor preparation

The protein HMGCR, with the PDB ID: 1HWJ, was obtained from the RCSB Protein Data Bank and its crystal structure was downloaded. To facilitate the docking analysis, AutoDockTools v.1.5.6 was utilized, with the necessary preferences being configured accordingly[19]. To streamline the process, all the chains of the protein except chain A were removed, focusing solely on chain A for subsequent docking analysis. Subsequently, water molecules and heteroatoms were removed from the structure. To ensure the completeness of the protein, missing atoms were repaired and the resulting structure was saved as two separate sets. To enhance the accuracy of the docking procedure, polar hydrogens were added to the prepared 1HWJ structure, and Gasteiger charges were assigned to the atoms. Finally, the fully prepared 1HWJ structure was saved as a PDBQT file, ready to be utilized in the docking process with the respective fatty acids.

Ligand preparation

The specific fatty acid amides required for the docking analysis were obtained from PubChem, and the 3D conformer of each fatty acid was obtained by downloading the corresponding SDF file. Open Babel v.2.4.1 was employed to convert the ligand file to PDBQT, which is compatible with AutoDockTools. Additionally, the ligand file underwent Gasteiger charge assignment to ensure accurate representation. In order to properly define the binding site and optimize the docking process, the 'Torsion Tree' feature was utilized. The 'Detect Root' option was applied to establish the suitable starting configuration for the ligand within the active site of the receptor.

Docking with AutoDock-GPU

Subsequently, AutoDockTools was utilized to prepare the docking input files for AutoDock. The parameters of the grid box were adjusted to ensure optimal coverage of the macromolecule and ligand, with the number of points in the x-, y-, and z-directions set to 126, a spacing of 0.375 Å, and the center of the macromolecule was -41.755Å, 60.694Å and -3.288Å, which was the binding site of endogenous ligand. To generate the grid maps required for docking calculations, AutoGrid was executed to generate the grid maps required for docking calculations. AutoDock-GPU was employed for docking, utilizing the Lamarckian Genetic Algorithm (LGA) and ADADELTA gradient-based local search methods for conformation search algorithms[20]. The energy-based scoring function was used to measure the quality of a given binding pose. The docking parameters were set as follows: 50 GA runs with a population size of 300, 2500000 energy evaluations, and 27000 generations per LGA run. Upon the completion of the docking runs, the resulting DLG file was loaded into AutoDockTools for analysis. The RMSD table was examined to identify the run exhibiting the most negative binding energy, suggesting a potentially strong binding interaction. Open Babel was then used to convert the PDBQT file of the complex into a PDB file format, which was subsequently visualized through PLIP (Protein-Ligand Interaction Profiler)[21]. The resulting file of the complex was downloaded from PLIP and further visualized using PyMOL 2.5 software.

Data analysis and statistics

The data analysis and generation of graphs for the enzyme assay were conducted using GraphPad Prism version 5 (GraphPad Software, Inc., San Diego, CA, USA) software. Experiments were carried out in triplicate. Mean ± SD considered when generating graphs. The data were statistically examined using one-way ANOVA with Tukey's test to determine significant differences among the control group and fatty acid amide doses.

Results and Discussion

Figure 1 displays the spectrophotometric time scans displaying the progress of the reaction catalysed by HMGCR either in the presence or absence of three amides stearamide (A) oleamide (B) and butyramide (C). The enzyme inhibitions of stearamide, oleamide, and butyramide were determined at different two concentrations. At 25 µM, stearamide showed 34.98%±14.58 inhibition, oleamide showed 14.99%±4.10 inhibition, and butyramide showed

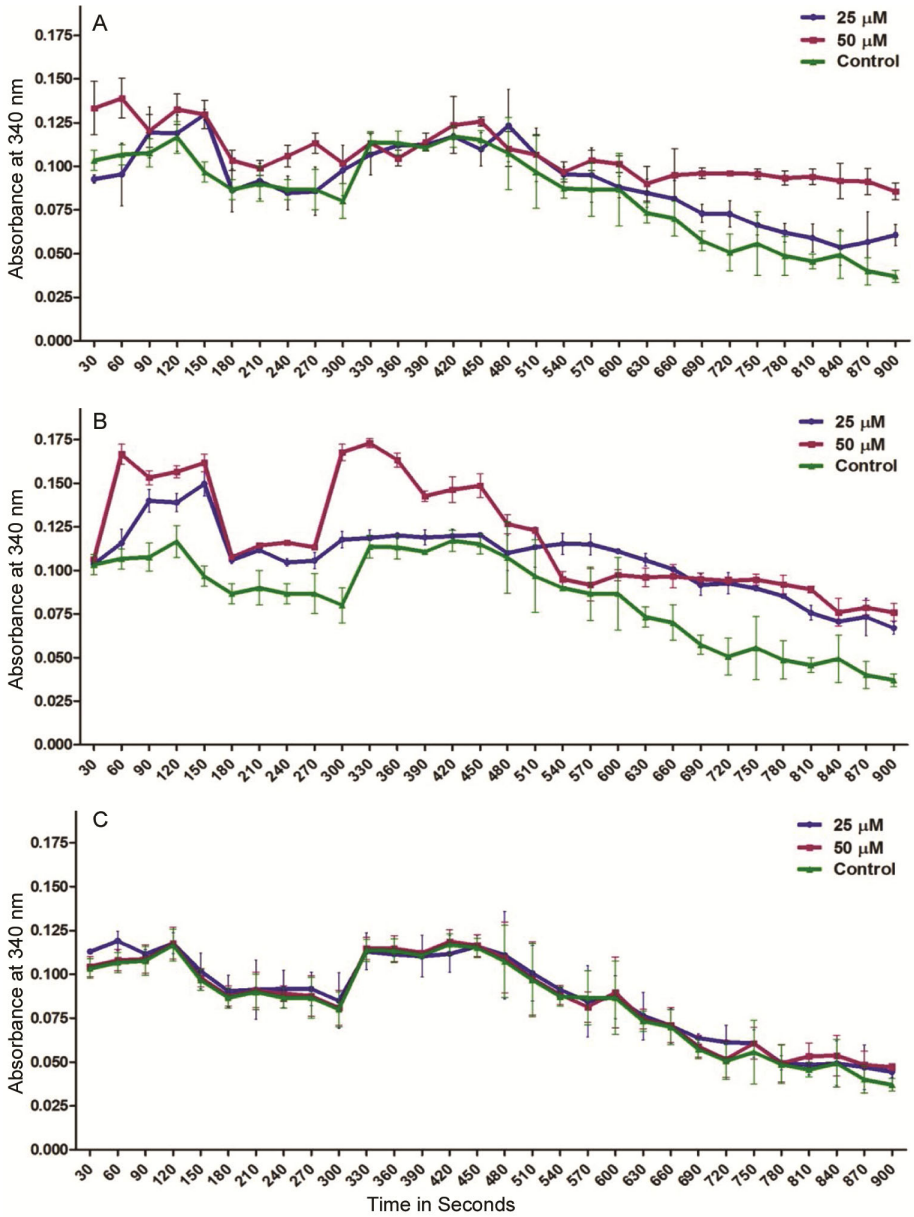

Fig. 1 — The spectrophotometric time scans displaying the progress of the reaction catalysed by HMGCR either in the presence or absence of (A) stearamide; (B) oleamide; and (C) butyramide tested at 25 and 50 µM doses. The assays were carried out in 96-well plates and the absorbance was recorded at 340 nm for 15 min at 30 sec time intervals. Bar mean ± SD (n = 3). Vehicle controls (negative controls) received only ethanol

14.46%±4.85 inhibition. At 50 µM concentration, stearamide displayed 78.65%±10.46 inhibition, oleamide displayed 63.70%±8.40 inhibition, and butyramide showed 22.43%±7.64 inhibition, confirming that stearamide has the greatest ability to inhibit the activity of HMGCR at tested doses (Fig. 2). Pravastatin, supplied with the kit, was used as the positive control. Pravastatin showed 61.06%±1.05 inhibition at 25 nM and nearly 88.14%±0.99 inhibition at 50 nM concentration (Fig. 2). According to enzyme kinetics (Fig. 3), stearamide appears to display a competitive mode of inhibition where V_{max} was almost unchanged (0.013 mM min^{-1}) for HMGCR in the reactions containing stearamide (25 µM) compared to the control. The K_m value for HMG-CoA for HMGCR in

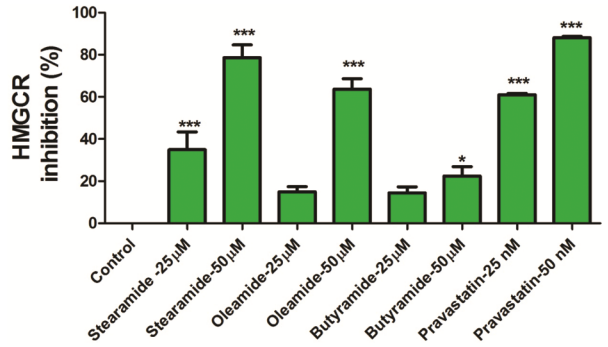

Fig. 2 — HMGCR inhibition percentages of stearamide, oleamide, butyramide and pravastatin. Data expressed as mean as ± SD. Statistical comparison among groups (control *vs* fatty acid amide doses) was carried out using one-way ANOVA with Tukey test with *P* value of <0.05

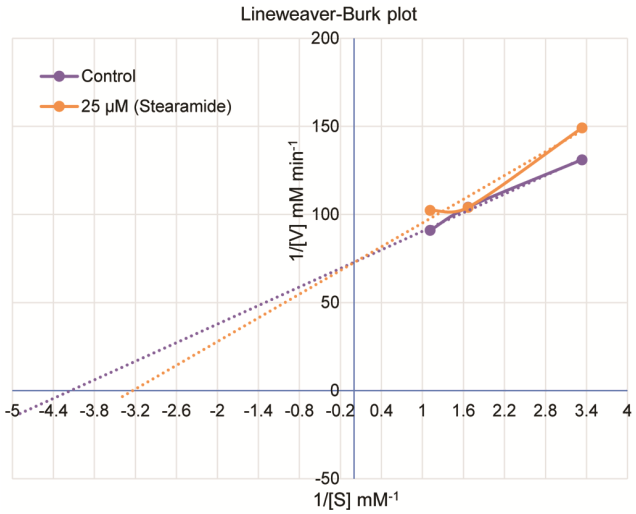

Fig. 3 — The Lineweaver-Burk plot analysis for HMGCR in the presence of different concentrations of HMG-CoA (0.3, 0.6 and 0.9 mM), the substrate of HMGCR, and stearamide (25 µM)

the presence of stearamide wes 0.30 mM, while in the absence of stearamide (control) it was 0.24 mM, indicating that stearamide exerts a competitive mode of inhibition (increasing K_m and no change in V_{max}) on HMGCR[1]. Enzyme kinetic studies with other amides oleamide and butyramide were not conducted in this study due to financial limitations experienced in purchasing kits. Therefore, the enzyme kinetic studies were only conducted for the amide (stearamide) which showed higher inhibitory potential.

The human HMGCR consists of a single polypeptide chain made up of 888 amino acids, which is divided into three main domains. The membrane anchor domain (residues 1-339) is located in the endoplasmic reticulum membrane, while the catalytic domain (residues 460-888) is found in the cytoplasm[22-24]. The linker region, comprising 340-459 amino acid residues, connects the membrane anchor domain and the catalytic domain of the enzyme. Within the catalytic domain, three subdomains (N, L, and S domains) have been identified[22-24]. The α-helical amino-terminal N-domain (residues 460-527) acts as a connection between the L domain and the linker domain. The L domain contains a region (residues 528-590 and 694-872) that binds to HMG-CoA, and the small carboxyl-terminal S-domain (residues 591-682) binds to NADPH. The cis-loop (residues 682-694), which links the L-domain and the S-domains, is crucial for the formation of the HMG-binding site and the NADPH-binding region[22-24].

According the crystal structures of the enzyme, the catalytic regions of the enzyme come together to form a tetramer with four identical monomers, with each active site positioned at the junction of two monomers. The functional unit of the enzyme is a homodimer. Interestingly, the formation of the tetramer does not appear to impact substrate binding. The active site of HMGCR is situated at the interface of the homodimer, where one monomer binds the nicotinamide dinucleotide and the other monomer binds the HMG-CoA[22-24]. The active site of HMGCR comprises three distinct binding subsites: one for HMG, one for CoA, and one for NADPH. The CoA binding pocket involves specific residues, namely Ser565, Asn567, Arg568, Lys722, Ser865, His866, and Tyr479, where last residue comes from an adjacent monomer. On the other hand, the NADPH binds to the S-domain of the opposing subunit, where the HMG-CoA binding pocket is situated. This binding event involves residues Ser626, Arg627, Phe628, Asp653, Met655, Gly656, Met657, Asn658,

Val805, as well as Asn870 and Arg871 from the neighbouring monomer[22-24]. Potential drug candidates that bind to the active site of this enzyme are considered potent HMGCR inhibitors[25].

The results of the molecular docking study of fatty acid amides bound to HMGCR are illustrated in (Fig. 4A-C). Based on the results of molecular docking, stearamide, oleamide, butyramide showed a binding energy of -4.62Kcal/mol, -4.39Kcal/mol and -3.96 Kcal/mol, respectively. Upon analysis, it was observed that stearamide (Fig. 4A) formed a hydrogen bond with Ala768. Additionally, several hydrophobic interactions were established between stearamide and Ala654, Met655, Asn658, and Thr809 residues. On the other hand, oleamide exhibited a single hydrogen bond with Pro813. Moreover, multiple hydrophobic interactions were observed between oleamide and Tyr517, Val522, Val530, Tyr533, Ile536 and Val538 residues (Fig. 4B). Butyramide formed hydrogen bonds with Gly808 and Thr809 residues. In addition,

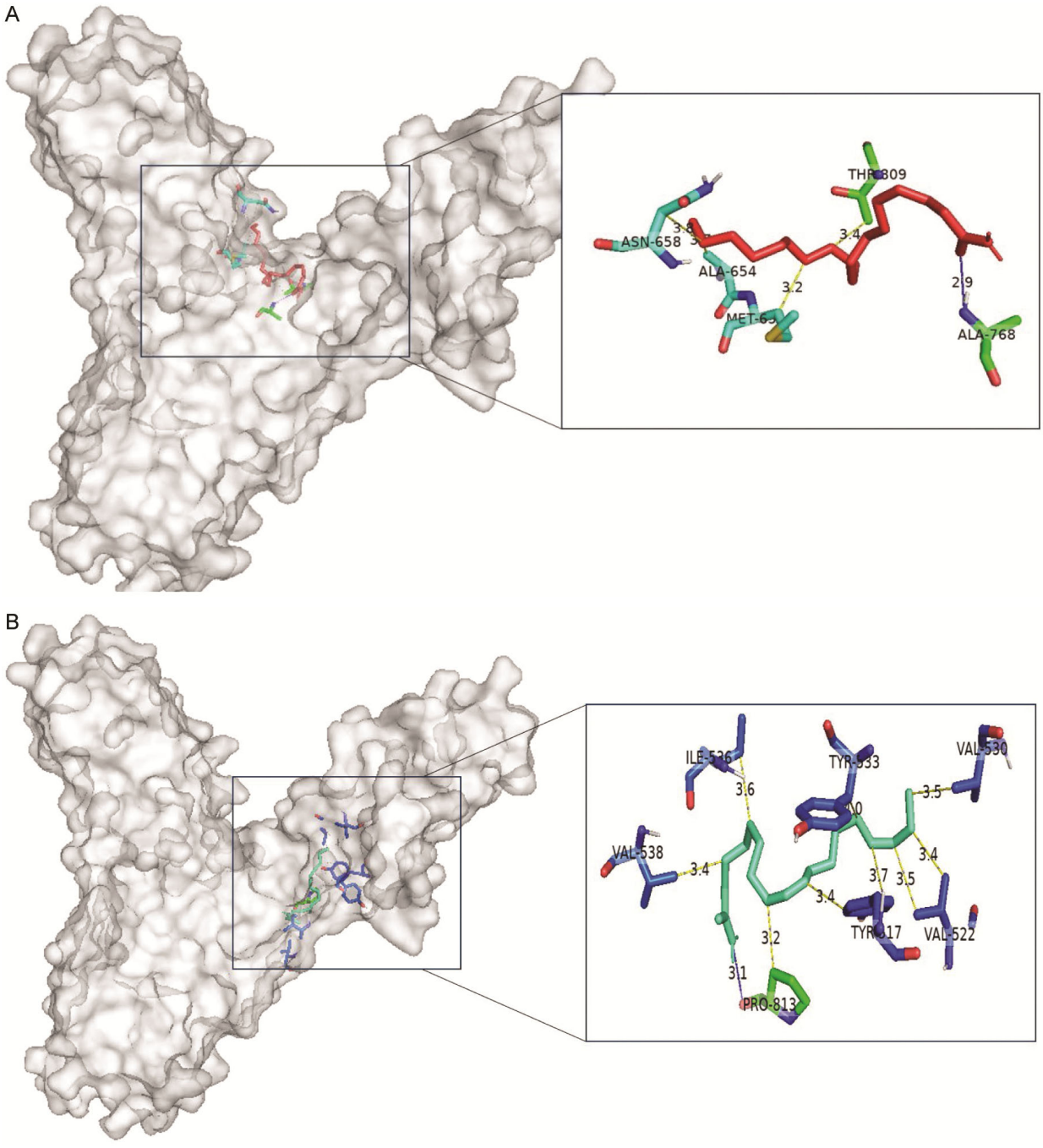

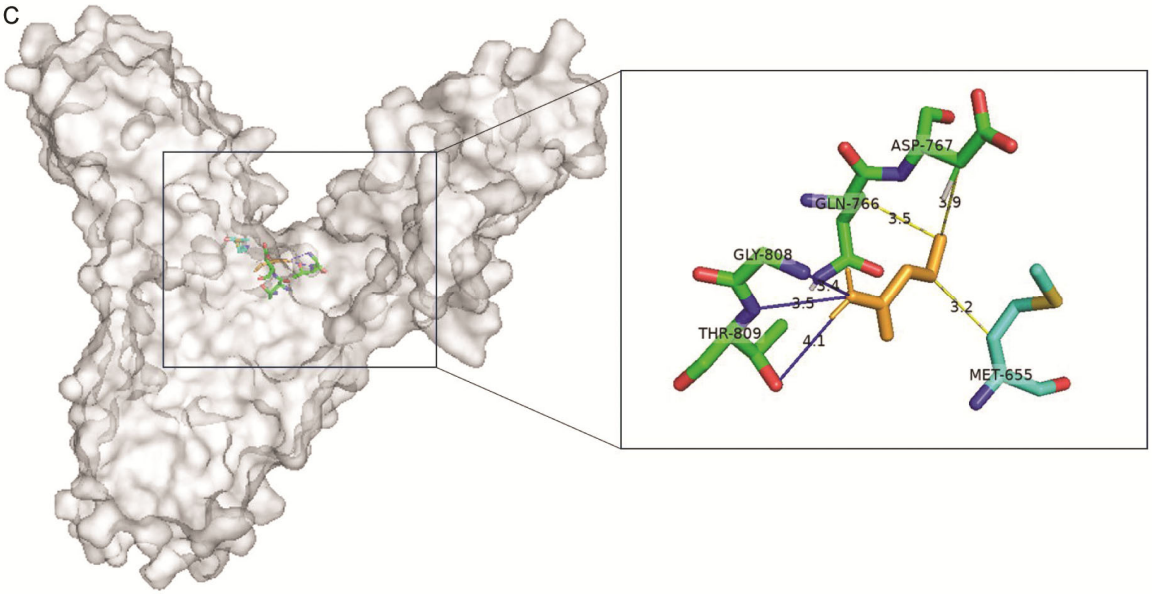

Fig. 4 — Visualization of the HMGCR receptor docking (PDB ID: 1HWJ) with fatty acid amides (A) stearamide; (B) oleamide; and (C) butyramide. Dark blue lines are hydrogen bonds, yellow lines are hydrophobic interactions

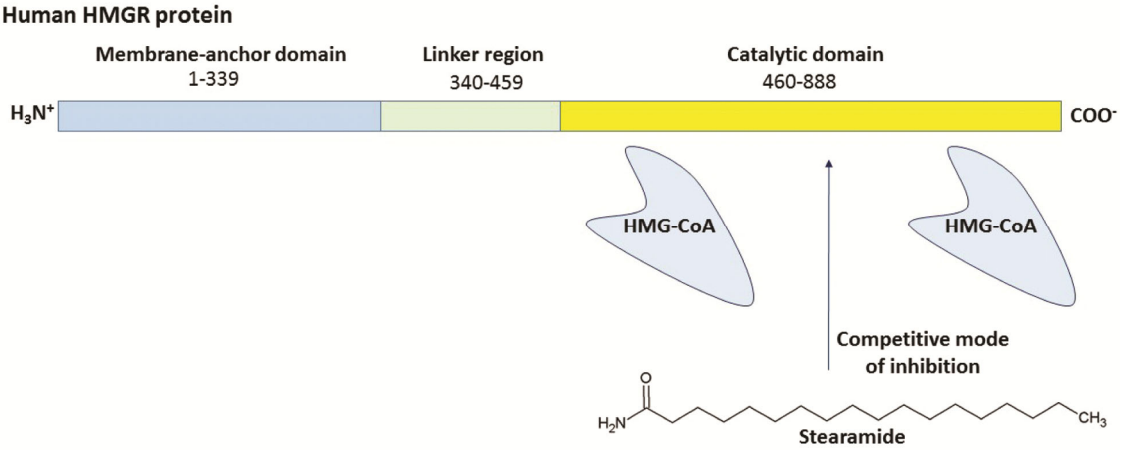

Fig. 5 — A schematic showing the mode of inhibition of stearamide on HMGCR. The human HMGCR is composed of a single polypeptide chain consisting of 888 amino acids, organized into three primary domains. The membrane anchor domain, which spans residues 1 to 339, is situated within the endoplasmic reticulum membrane. In contrast, the catalytic domain encompasses residues 460 to 888 and is located in the cytoplasm. Additionally, there is a linker region that includes amino acids 340 to 459. Stearamide seems to exhibit a competitive inhibition mechanism for HMGCR

several hydrophobic interactions were noted between butyramide and Met655, Gln766, and Asp767 residues (Fig. 4C).

According to interaction analysis, three fatty acid amides showed several hydrophobic bindings in the catalytic portion (residues 426-888), proposing the blockade of the access of the substrate, HMG-CoA, and confirm the role of these three fatty acid amides on the activity of the enzyme. It is interesting to note that butyramide forms a hydrophobic interaction with Asp767, which is in catalytic site of the enzyme[23]. In addition, we hypothesize that the increased number of carbons in the side chains of stearamide (17 carbons) and oleamide (17 carbons), as opposed to butyramide (3 carbons), contributes to their enhanced binding affinities through hydrophobic interactions. Stearamide seems to exhibit a competitive inhibition mechanism, as indicated by the nearly unchanged V_{max} (0.013 mM min^{-1}) for HMGCR when stearamide (25 µM) is used, in comparison to the control (Fig. 3). A schematic illustrating this mode of inhibition is provided in (Fig. 5). A recent investigation highlights the significant role of hydrophobic interactions in inhibiting the activity of the HMGCR. This inhibition

is achieved by natural compounds, such as geranylgeraniol, phytol, and farnesyl acetate, which possess lengthy non-polar side chains, similar to those found in fatty acid amides[26,27]. Factors such as charge, hydrophobicity, hydrophilicity, and conformational changes affect the binding of drugs to proteins[28]. These factors can be assessed through molecular dynamic simulations[29], and we plan to conduct this in our future studies depending on our funding status, using a series of fatty acid amides. Statins, widely used cholesterol-lowering drugs, inhibit the activity of HMGCR. However, long-term usage of statins is associated with unfavourable side effects[30]. This investigation explores fatty acid amides as potential alternatives to statins for HMG-CoA reductase inhibition, which might has the potential to pave the way for the development of improved cholesterol-lowering medications.

Conclusion

This preliminary investigation of stearamide, oleamide, and butyramide as HMGCR inhibitors discloses their potential, with stearamide exhibiting the highest inhibitory potency. Further research exploring the effects of fatty acid amides on HMGCR inhibition in *in vivo* models is warranted. This investigation further directs the potential combination/s of fatty acid amides and statins, which could offer valuable insights in the area of cholesterol lowering drug discovery strategies.

Acknowledgement

The present study was supported by grants from the UNESCO-TWAS and the Swedish International Development Cooperation Agency (Grant number 22-140 RG/BIO/AS_I).

Conflicts of interest

All authors declare no conflicts of interest.

References

1 Pak VV, Khojimatov OK, Pak AV & Sagdullaev SS, Design of competitive inhibitory peptides for HMG-CoA reductase and modeling structural preference for short linear peptides. *J Mol Struct*, 1261 (2022) 132909.

2 Ezzili C, Otrubova K & Boger DL, Fatty acid amide signaling molecules. *Bioorg Med Chem Lett*, 20 (2010) 5959.

3 Arafat ES, Trimble JW, Andersen RN, Dass C & Desiderio DM, Identification of fatty acid amides in human plasma. *Life Sci*, 45 (1989) 1679.

4 Kim M, Snowden S, Suvitaival T, Ali A, Merkler DJ, Ahmad T, Westwood S, Baird A, Proitsi P, Nevado-Holgado A & Hye A, Primary fatty amides in plasma associated with brain amyloid burden, hippocampal volume, and memory in the European medical information framework for Alzheimer's disease biomarker discovery cohort. *Alzheimers Dement*, 15 (2019) 817.

5 Bisogno T, Katayama K, Melck D, Ueda N, De Petrocellis L, Yamamoto S & Di Marzo V, Biosynthesis and degradation of bioactive fatty acid amides in human breast cancer and rat pheochromocytoma cells: implications for cell proliferation and differentiation. *Eur J Biochem*, 254 (1998) 634.

6 Nichols KK, Ham BM, Nichols JJ, Ziegler C & Green-Church KB, Identification of fatty acids and fatty acid amides in human meibomian gland secretions. *Invest Ophthalmol Vis Sci*, 48 (2007) 34.

7 Yang WS, Lee SR, Jeong YJ, Park DW, Cho YM, Joo HM, Kim I, Seu YB, Sohn EH & Kang SC, Antiallergic activity of ethanol extracts of *Arctium lappa* L. undried roots and its active compound, oleamide, in regulating FcεRI-mediated and MAPK signaling in RBL-2H3 cells. *J Agric Food Chem*, 64 (2016) 3564.

8 Mendelson WB & Basile AS, The hypnotic actions of the fatty acid amide, oleamide. *Neuropsychopharmacology*, 25 (2001) S36-9.

9 Boger DL, Patterson JE, Guan X, Cravatt BF, Lerner RA & Gilula NB, Chemical requirements for inhibition of gap junction communication by the biologically active lipid oleamide. *Proc Natl Acad Sci U S A*, 95 (1998a) 4810.

10 Boger DL, Patterson JE & Jin Q, Structural requirements for 5-HT2A and 5-HT1A serotonin receptor potentiation by the biologically active lipid oleamide. *Proc Natl Acad Sci U S A*, 95 (1998b) 4102.

11 Reyes-Soto CY, Villaseca-Flores M, Ovalle-Noguez EA, Nava-Osorio J, Galván-Arzate S, Rangel-López E, Maya-López M, Retana-Márquez S, Túnez I, Tinkov AA & Ke T, Oleamide Reduces Mitochondrial Dysfunction and Toxicity in Rat Cortical Slices Through the Combined Action of Cannabinoid Receptors Activation and Induction of Antioxidant Activity. *Neurotox Res*, 40 (2022) 2167.

12 Kim YA, Lee SH, Koh JM, Kwon SH, Lee Y, Cho HJ, Kim H, Kim SJ, Lee JH, Yoo HJ & Seo JH, Fatty acid amides as potential circulating biomarkers for sarcopenia. *J Cachexia Sarcopenia Muscle*, 14 (2023) 1558.

13 Ahmed S, Liu H, Ahmad A, Akram W, Abdelrahman EK, Ran F, Ou W, Dong S, Cai Q, Zhang Q & Li X, Characterization of anti-bacterial compounds from the seed coat of Chinese windmill palm tree (*Trachycarpus fortunei*). *Front Microbiol*, 8 (2017) 1894.

14 Jiang-shan LI, Wei L, Shao-rui H, Yong-zheng G, Hai-jun H, De-ying C, Qing XI, Xiao-ping P, Wei XU, Wen-xia Y & Lan-juan L, A serum metabonomic study on the difference between alcohol-and HBV-induced liver cirrhosis by ultraperformance liquid chromatography coupled to mass spectrometry plus quadrupole time-of-flight mass spectrometry. *Chin Med J (Engl)*, 124 (2011) 1367.

15 Steliou K, Boosalis MS, Perrine SP, Sangerman J & Faller DV, Butyrate histone deacetylase inhibitors. *BioRes Open Access*, 1 (2012) 192.

16 Grande F, Anderson JT & Keys A, Phenyl butyramide and the serum cholesterol concentration in man. *Metabolism*, 6 (1957) 154.

17 Iqbal D, Khan MS, Khan MS, Ahmad S, Hussain MS & Ali M, Bioactivity guided fractionation and hypolipidemic

property of a novel HMG-CoA reductase inhibitor from *Ficus virens* Ait. *Lipids Health Dis*, 14 (2015) 1.

18 Heres A, Mora L & Toldrá F, Inhibition of 3-hydroxy-3-methyl-glutaryl-coenzyme A reductase enzyme by dipeptides identified in dry-cured ham. *Food Prod Process Nutr*, 3 (2021) 1.

19 Forli S, Huey R, Pique ME, Sanner MF, Goodsell DS & Olson AJ, Computational protein–ligand docking and virtual drug screening with the AutoDock suite. *Nat Protoc*, 11 (2016) 905.

20 Santos-Martins D, Solis-Vasquez L, Tillack AF, Sanner MF, Koch A & Forli S, Accelerating AutoDock4 with GPUs and gradient-based local search. *J Chem Theory Comput*, 17 (2021) 1060.

21 Adasme MF, Linnemann KL, Bolz SN, Kaiser F, Salentin S, Haupt VJ & Schroeder M, PLIP 2021: Expanding the scope of the protein–ligand interaction profiler to DNA and RNA. *Nucleic Acids Res*, 49 (2021) 530.

22 Friesen JA & Rodwell VW, The 3-hydroxy-3-methylglutaryl coenzyme-A (HMG-CoA) reductases. *Genome Biol*, 5 (2004) 1.

23 Gesto DS, Pereira CM, Cerqueira NM & Sousa SF, An atomic-level perspective of HMG-CoA- reductase: The target enzyme to treat hypercholesterolemia. *Molecules*, 25 (2020) 3891.

24 Istvan ES & Deisenhofer J, Structural mechanism for statin inhibition of HMG-CoA reductase, *Science* 292 (2001) 1160.

25 Son M, Baek A, Sakkiah S, Park C, John S & Lee KW, Exploration of virtual candidates for human HMG-CoA reductase inhibitors using pharmacophore modeling and molecular dynamics simulations. *PLoS One*, 8 (2013) e83496.

26 Ramírez-Santos J, Calzada F, Mendieta-Wejebe JE, Ordoñez-Razo RM, Martinez-Casares RM & Valdes M, Understanding the antilymphoma activity of *Annona macroprophyllata* Donn and its acyclic terpenoids: *In vivo*, *In vitro*, and *In silico* studies. *Molecules*, 27 (2022) 7123.

27 Almalki SG, Alsaweed M, MutebAlbadrani H, Alqurashi YE, Bazuhair MA, Ahmed HH, Ahmad P, Alfahed A, Al Othaim A & Iqbal D, A molecular informatics and *in vitro* approach to evaluate the HMG-CoA reductase inhibitory efficacy of monoterpenes, carvacrol and geraniol. *J Taibah Univ Sci*, 8 (2024) 2297456.

28 Siebenmorgen T & Zacharias M, Computational prediction of protein–protein binding affinities. *Wiley Interdiscip Rev Comput Mol Sci*, 10 (2020) 1448.

29 Erdogan T, Computational evaluation of 2-arylbenzofurans for their potential use against SARS-CoV-2: A DFT, molecular docking, molecular dynamics simulation study. *Indian J Biochem Biophys*, 59 (2022) 59.

30 ToppoAL, Yadav M, Dhagat S, Ayothiraman S & Jujjavarapu SE, Molecular docking and ADMET analysis of synthetic statins for HMG-CoA reductase inhibition activity. *Indian J Biochem Biophys*, 58 (2021) 127.